Bulgarian Chemical Communications, Volume 47, Special Issue B (pp. 200–207) 2015

A feasibility study of hyperon measurements in Au-Au collisions at NICA/MPD

D. Suvarieva*, M. Ilieva, V. Kolesnikov, V. Vasendina, A. Zinchenko

Veksler and Baldin Laboratory of High Energy Physics, Joint Institute for Nuclear Research, 141980 Dubna, Moscow region, Russia

One of the main tasks of NICA/MPD physics program is a study of the strangeness production in nuclear collisions. In this paper the MPD detector performance for measurements of Λ, Ξ^- and Ω^- hyperons in central Au+Au collisions at NICA energies is presented. The investigation has been performed at the Laboratory of High Energy Physics, JINR.

Key words: hyperons, strangeness production, heavy-ion collisions, NICA/MPD

INTRODUCTION

The main goal of studying heavy-ion collisions is to explore the properties of nuclear matter under extreme density and temperature conditions. Production of strange particles is of particular interest because enhanced production of rare strange hadrons (Ξ^-, Ω^-) in A+A collisions (relative to the yields from elementary pp reactions) was predicted as a signal for the QGP formation [1].

At present, a complete theoretical description of the (multi)strangeness production mechanism at collision energies ($\sqrt{s}$) of several GeV, has not yet been achieved. In order to better understand the dynamics of hot and dense hadronic matter the MPD experiment at NICA [2] will provide new precise experimental data on the total yields, rapidity, transverse momentum, and azimuthal angle distributions of hyperons The production of baryons and antibaryons with different strangeness content produced in central heavy ion collisions will be compared with those produced in proton induced reactions where no QGP formation is expected.

The goal of this study is to evaluate the performance of the MPD detector for reconstruction of hyperons in Au+Au collisions.

* To whom all correspondence should be sent:
DilyanaSuvarieva@mail.bg

MPD at NICA

The Nuclotron-based Ion Collider fAcility (NICA) [3], shown in Fig. 1, is a new accelerator complex being constructed at JINR, Dubna, Russia. NICA's aim is to provide collisions of heavy ions over a wide range of atomic masses, from Au+Au collisions at $\sqrt{s} = 4$–11A GeV (for Au^{79+}) and an average luminosity of $L = 10^{27}$ cm^{-2}s^{-1} to proton-proton collisions with $\sqrt{s_{pp}} = 20$ GeV and $L = 10^{32}$ cm^{-2}s^{-1}.

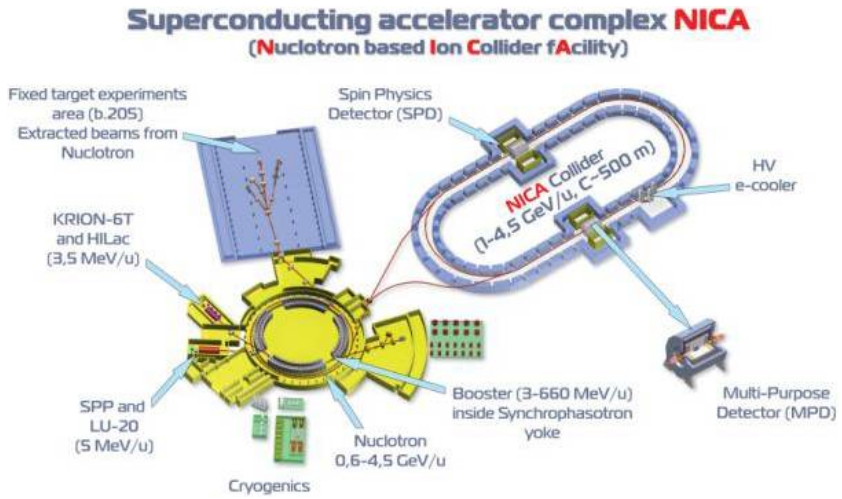

Fig. 1. NICA complex.

Two interaction points are foreseen at NICA which provide a possibility for two detectors to operate simultaneously – MultiPurpose Detector (MPD) and Spin Physics Detector (SPD).

The main goal of the NICA/MPD program [4] is a comprehensive experimental investigation of the properties and dynamics of the hot and dense nuclear matter in a poorly explored region of the QCD phase diagram, with a main emphasis to such QCD subjects as properties of deconfinement phase transition, critical phenomena and chiral symmetry restoration.

The NICA/MPD experimental program includes simultaneous measurements of observables that are presumably sensitive to high nuclear density effects and phase transitions. In the first stage of the project are considered – multiplicity and spectral characteristics of the identified hadrons including strange particles, multi-strange baryons and antibaryons; event-by-event fluctuations in multiplicity, charges and transverse momentum; collective flows (directed, elliptic and higher ones) for observed hadrons. In the second stage the electromagnetic probes (photons and dileptons) will be measured. It is proposed that along with heavy ions NICA will provide proton and light ion beams including the possibility to use polarized beams. Study of heavy ion collisions at the collider will be complemented by spin physics research with polarized beams of protons and deuterons as well as collisions in a fixed-target mode at center of mass energy from 1 to 4 GeV.

The detector for exploring phase diagram of strongly interacting matter in a high track multiplicity environment has to cover a large phase space, be functional at high interaction rates and comprise high efficiency and excellent particle identification capabilities. The MPD detector [2, 5], shown in Fig. 2, matches all these requirements. It consists of central detector (CD) and two optional forward spectrometers (FS-A and FS-B). CD consists of a barrel part and two end caps. The barrel part is a set of various subdetectors. The main tracker is the time projection chamber (TPC) supplemented by the inner tracker (IT). IT and TPC have to provide precise tracking, momentum determination and vertex reconstruction. The time of flight (TOF) system must be able to identify charged hadrons and nuclear clusters in a broad pseudorapidity range. The electromagnetic calorimeter (ECAL) should identify electrons, photons and measure their energy with high precision. The zero degree calorimeter (ZDC) should provide event centrality and event plane determination, and also measurement of the energy deposited by spectators. There are also a straw-tube tracker (ECT) and a fast forward detector (FFD).

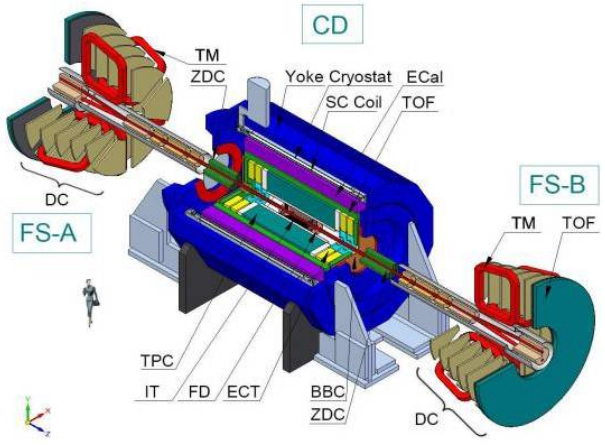

Fig. 2. MPD detector.

The magnet of MPD is a solenoid with a thin superconducting NbTi winding and a flux return iron yoke. The magnet should provide a homogeneous magnetic field of 0.5 T. The field inhomogeneity in the tracker area of the detector is about 0.1%.

The MPD time projection chamber (TPC) is the main tracking detector of the central barrel and has to provide charged particles momentum measurement with sufficient resolution (about 2% at $p_t =$ 300 MeV/c), particle identification and vertex determination, two track separation (with a resolution < 1 cm) and dE/dx measurement (dE/dx resolution better than 8%) for hadronic and leptonic observables at pseudorapidities $|\eta| < 2.0$ and $p_t > 100$ MeV/c. TPC readout system is based on Multi-Wire Proportional Chambers (MWPC) with cathode readout pads.

The identification of charged hadrons (PID) at intermediate momentum (0.1-3 GeV/c) is achieved by the time-of-flight (TOF) measurements which are complemented by the energy loss (dE/dx) information from the TPC and IT detector systems. TOF system should provide a large phase space coverage $|\eta| < 3.0$, high combined geometrical and detection efficiency (better than 80%), identification of pions and kaons with $0.1 < p_t < 2$ GeV/c and (anti)protons with $0.3 < p_t < 3$ GeV/c. The choice for the TOF system is Multigap Resistive Plate Counters (MRPC) which have good time resolution of $\sigma < 70$ ps. The barrel covers the pseudorapidity region $|\eta| < 1.5$ and the geometry efficiency in it is above 90%. The end cap system covers the pseudorapidity region $1.5 < |\eta| < 3.0$.

EVENT GENERATORS AND DATA SETS

The software framework for the MPD experiment (MpdRoot [6]) is based on FairRoot and provides a powerful tool for detector performance studies, development of algorithms for reconstruction and physics analysis of the data [2]. The event samples used for the present study were produced with the UrQMD [7] generator at $\sqrt{s} = 9$A GeV.

Produced by the event generators particles have been transported through the detector using the GEANT3 transport package (describing particle decays, secondary interactions, etc.). It should be noted here that the overall detector material budget is dominated by the contribution from the TPC inner and outer cages which are multilayer structures made of composite materials like kevlar and tedlar with high strength and long radiation length. As a result, the total amount of the material does not exceed 10% of the radiation length in the region of interest.

DETECTOR PERFORMANCE

Track reconstruction

The track reconstruction method is based on the Kalman filtering technique (see, e.g. [8]) and the number of TPC points per track was required to be greater than 10 to ensure a good precision of momentum and dE/dx measurements. In addition, we have restricted our study to the mid-rapidity region with $|\eta| < 1.3$. The track finding efficiency in TPC for primary and secondary tracks is shown in Fig. 3 (a) as a function of the track transverse momentum. The secondary track sample there included particles produced within 50 cm of the primary vertex both in transverse and longitudinal directions and did not include electrons and positrons from the photon conversion, which are not relevant for the current study. The transverse momentum resolution as a function of p_T can be seen on Fig. 3 (b). The result has been obtained with the assumption on the TPC coordinate resolution of 0.5 and 1.0 mm in transverse and longitudinal directions, respectively. Fig. 4(a) shows the transverse and longitudinal position uncertainties of primary tracks at their point of the closest approach to the interaction point versus track momentum. These detector characteristics are important for secondary vertex reconstruction.

Both the primary and secondary vertex reconstruction methods utilized make use of the similar approach based on the Kalman filtering formalism [9]. The primary vertex reconstruction errors as functions of the track multiplicity in the event are shown in Fig. 4(b).

For all the reconstructed in the TPC tracks the specific energy loss dE/dx is calculated as a truncated mean of the charges of TPC hits assigned to the tracks. The truncation level of 70% was chosen, i.e. 30% of hits with the highest charges were excluded from the mean value.

Next, the TPC reconstructed tracks are extrapolated to the TOF detector and matched to the TOF hits. For the matched candidates the mass square (M^2) is derived through the relation:

$$M^2 = (p/q)^2 \left(\frac{c^2 t^2}{l^2} - 1 \right)$$

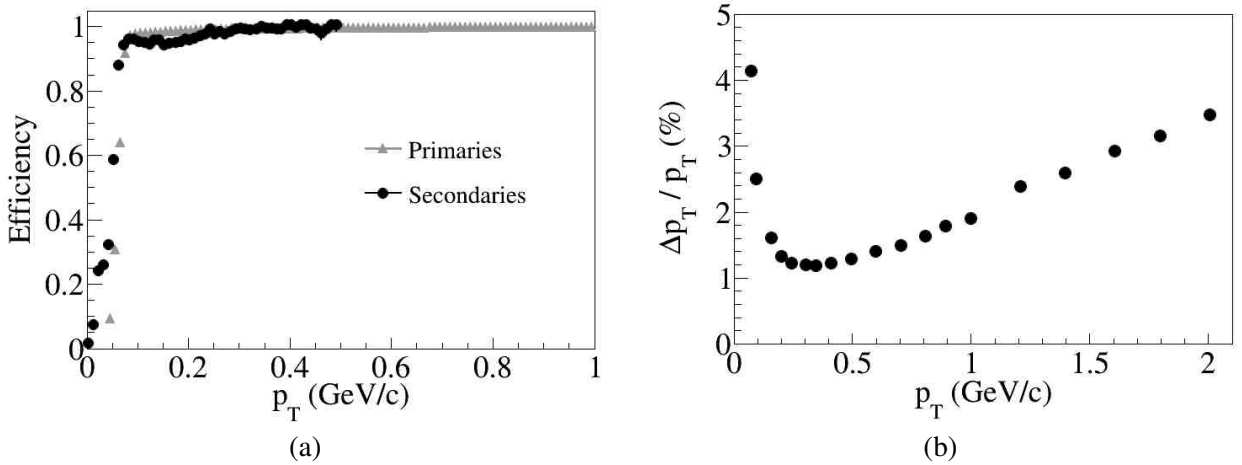

(a) (b)

Fig. 3. (a) – track reconstruction efficiency as a function of track p_T for primary and secondary particles; (b) – relative transverse momentum resolution for primary tracks with $|\eta| < 1.3$ reconstructed in TPC.

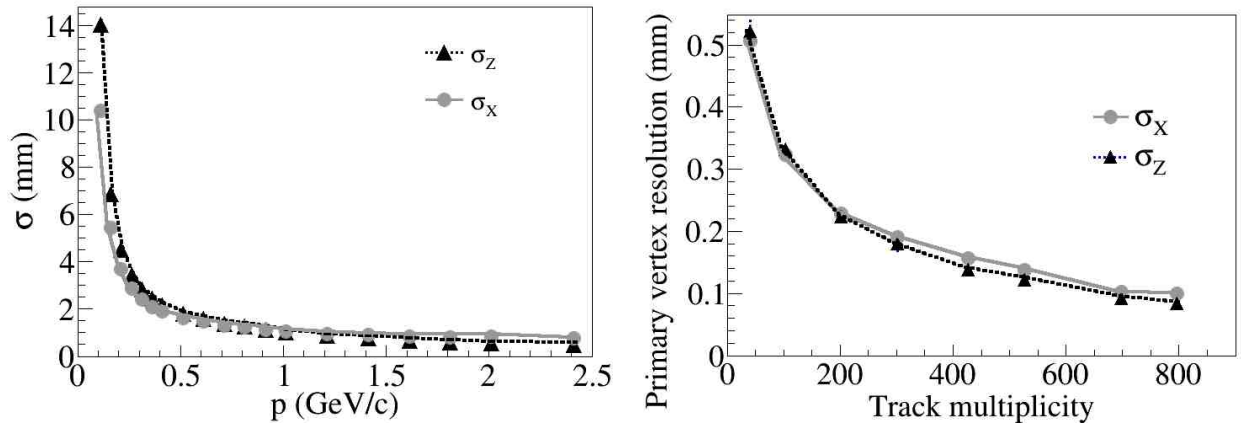

(a) (b)

Fig. 4. (a) – transverse and longitudinal position errors in the point of the closest approach (PCA) to the interaction point for TPC reconstructed primary tracks with $|\eta| < 1.3$ versus particle momentum; (b) – transverse and longitudinal position errors of the reconstructed primary vertex as functions of track multiplicity.

where p is the track momentum, q is its charge, t is the time-of-flight from TOF, l is the path length from the collision vertex to the TOF hit, and c is the speed of light. p/q, so-called magnetic rigidity, is the value directly returned by the track reconstruction algorithm. For particles with the unit charge it is equal to the momentum and M^2 corresponds to the particle mass, whereas for multiple-charged particles the obtained value of M^2 is scaled by the factor of $1/q^2$ with respect to the true mass.

Particle identification

Particle identification (PID) in the MPD experiment will be achieved by combining specific energy loss (dE/dx) and time-of-flight measurements. The basic detector parameters, namely, dE/dx and TOF resolutions of $\sigma_{dE/dx} \approx 6\%$ and $\sigma_{TOF} \approx 100$ ps will provide a high degree of selectivity for hadrons at momenta below 2 GeV/c (see Fig. 5).

An identified hadron candidate is assumed to lie within the boundaries of the PID ellipse (3σ around the nominal position for a given particle specie). In addition, the probability for a given particle to belong to each of the species can be calculated knowing the widths of the corresponding distributions (along the dE/dx and M^2 axes) and the difference from the predicted position for the specie. It was found that by requiring this probability to be greater than 0.75 one can get distributions for the PID efficiency and contamination (of wrongly identified hadrons) shown in Fig. 6. The PID efficiency is defined as a ratio of correctly tagged to the total number of generated particles.

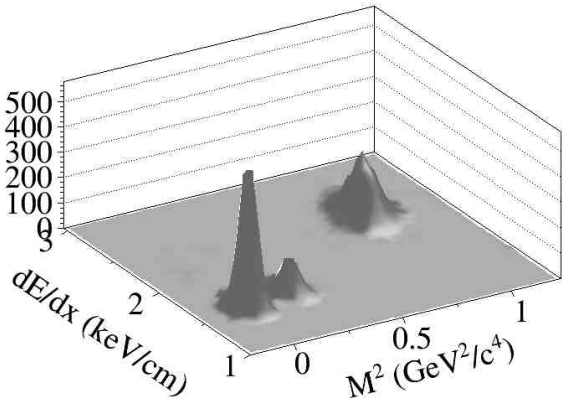

Fig. 5. A typical distribution of the specific energy loss dE/dx versus mass-squared for π^-, K^-, and protons (from left to right) at $p = 1$ GeV/c.

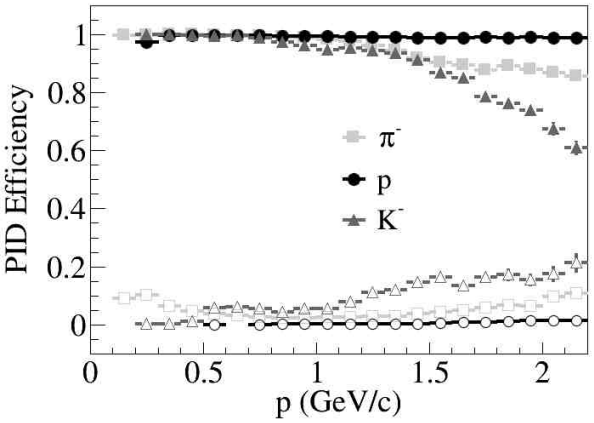

Fig. 6. PID efficiency (filled symbols) and contamination of wrongly identified particles (empty symbols) as a function of their total momentum.

The contamination is determined as the number of incorrectly tagged particles divided by the number of correctly tagged particles.

As can be seen from Fig. 6, the PID efficiency for protons is close to 1.0, while due to a partial overlap of the distributions for pions and kaons at high momenta, the efficiency of charged kaons drops down to ≈ 0.6 at $p = 2.5$ GeV/c.

ANALYSIS PROCEDURE

Multistrange hyperons were reconstructed using their decay modes into a charged particle and a Λ hyperon followed by Λ decay into a proton and a pion. The topologies of hyperon decays are shown in Fig. 7.

The event topology (decay of a relatively long-lived particle into two particles) defines the selection criteria: relatively large distance of the closest approach (*DCA*) to the primary vertex of decay products, small track-to-track separation in the decay vertex, relatively large decay length of the mother particle. Moreover, both the *DCA* and two-track separation cuts should be more efficient if applied in χ^2 - space, i.e if normalized to their respective errors.

The exact values of selection cuts were found by performing a multidimensional scan over the whole set of selection criteria with a requirement to maximize the invariant mass peak significance, defined as $S/\sqrt{S+B}$, where S and B are total numbers of signal (described the gaussian) and background (polynomial function) combinations inside $\pm 2\sigma$ interval around the peak position. While different physics analyses might prefer different selection quality criteria, the significance looks convenient to quantitatively evaluate effect of different factors on the reconstruction quality.

The corresponding scan procedure was realized as follows: during the particle combinations the parameters which have been chosen to serve as selection criteria (see above) were recorded along with the invariant mass value. Later, multiple loops over those variables were performed in some steps and their values were used as low or high thresholds, yielding the invariant mass peak significance for each set of selection cut values. Then, the maximum value was taken along with the corresponding set of selection parameters.

RESULTS AND DISCUSSION

Reconstruction of Λ hyperons

The results (Table 1 and Fig. 8) have been obtained for 10^4 central events, corresponding to about 30 seconds of data taking time.

Table 1. Factors affecting Λ reconstruction efficiency

Factor	Efficiency, %
Branching ratio: $\Lambda \to p + \pi^-$	63.4
p and π^- at $\lvert\eta\rvert < 1.3$	29.9
p and π^- at $\lvert\eta\rvert < 1.3$ and $p_T > 0.05$ GeV/c	28.3
p and π^- at $\lvert\eta\rvert < 1.3$ and $p_T > 0.1$ GeV/c	22.0
p and π^- at $\lvert\eta\rvert < 1.3$ and $p_T > 0.2$ GeV/c	8.6
Reconstructed p and π^- at $\lvert\eta\rvert < 1.3$	22.7
Maximum siginificance	8.6

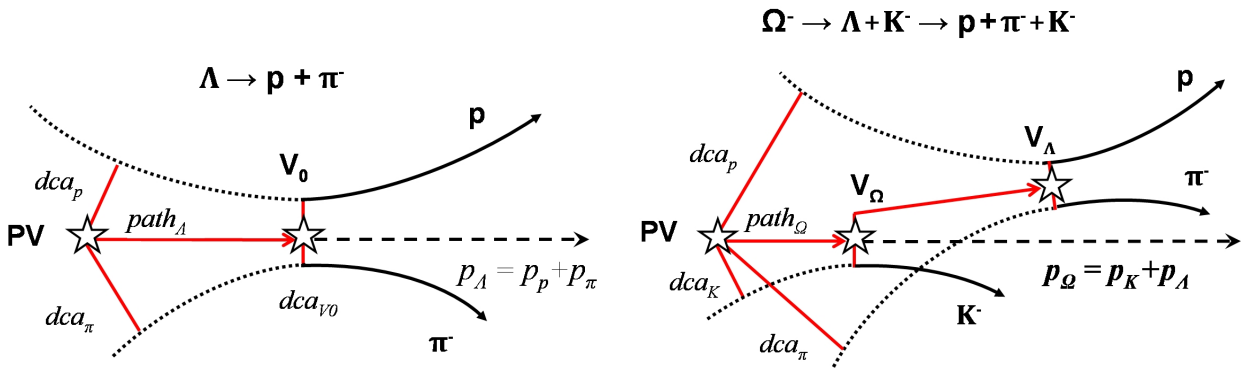

(a) (b)

Fig. 7. (a) – event topology of two-particle decays of a neutral particle (e.g. $\Lambda \to p + \pi^-$); (b) – event topology of cascade-type decays (e.g. $\Omega^- \to \Lambda + K^- \to p + \pi^- + K^-$) (transverse view). Here dca_p, dca_π and dca_K are the distances of the closest approach of the decay tracks to the primary vertex PV, dca_{V0} is the distance between daughter tracks in the decay vertex V_0, $path$ is the decay length, $\mathbf{p_p}$, $\mathbf{p_\pi}$, $\mathbf{p_K}$, p_Λ and p_Ω are momenta of particles.

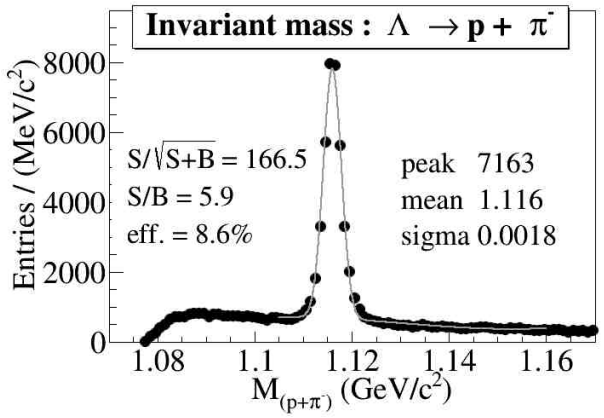

Fig. 8. Reconstructed invariant mass of proton and π^-.

Table 1 shows the effect of the detector acceptance (i.e. η-coverage and low-p_T cut for Λ decay products) on hyperon detection efficiency where the efficiency is defined with respect to the total number of hyperons. Lines 2-5 demonstrate the effect of the p_T-cut on the efficiency, where p_T is the true transverse momentum of the decay pion and proton. Line 6 shows the reconstruction efficiency, i.e. considering the reconstructed in the detector decay pions and protons without any explicit p_T-cut (and without PID efficiency). The last line includes all the relevant factors, i.e. reconstruction and PID efficiencies as well as selection efficiency. One can see that the detector provides efficient reconstruction of hyperons with p_T of decay tracks above 0.1 GeV/c in good agreement with Fig. 3. It is clear also that a higher p_T-threshold (e.g. 0.2 GeV/c) would significantly reduce the detector efficiency. The efficiency drop due to selection cuts comes from the necessity to suppress the combinatorial background in order to obtain a clean invariant mass peak.

Reconstruction of Ξ^- hyperons

The results (Table 2 and Fig. 9) have been obtained for $4 \cdot 10^4$ central events, corresponding to about 2 minutes of running time at the NICA collision rate of 6 kHz. Here, Λ-candidates in the invariant mass interval $\pm 3\sigma$ around the peak position were combined with negative pions to form Ξ^--candidates. In the selection procedure, additional acceptance cuts

Table 2. Factors affecting Ξ^- reconstruction efficiency

Factor	Efficiency %
Branching ratio: $\Xi^- \to \Lambda + \pi^-$ ($\Lambda \to p + \pi^-$)	63.6
p, π^- and π^- at $\|\eta\| < 1.3$	27.2
p, π^- and π^- at $\|\eta\| < 1.3$ and $p_T > 0.05$ GeV/c	24.6
p, π^- and π^- at $\|\eta\| < 1.3$ and $p_T > 0.1$ GeV/c	15.0
p, π^- and π^- at $\|\eta\| < 1.3$ and $p_T > 0.2$ GeV/c	2.9
Reconstructed p, π^- and π^- at $\|\eta\| < 1.3$	16.3
Maximum siginificance	2.5

Table 3. Factors affecting Ω^- reconstruction efficiency

Factor %	Efficiency
Branching ratio: $\Omega^- \to \Lambda + K^-$ ($\Lambda \to p + \pi^-$)	42.8
p, π^- and K^- at $\|\eta\| < 1.3$	18.4
p, π^- and K^- at $\|\eta\| < 1.3$ and $p_T > 0.05$ GeV/c	17.2
p, π^- and K^- at $\|\eta\| < 1.3$ and $p_T > 0.1$ GeV/c	12.2
p, π^- and K^- at $\|\eta\| < 1.3$ and $p_T > 0.2$ GeV/c	3.6
Reconstructed p, π^- and K^- at $\|\eta\| < 1.3$	10.0
Maximum siginificance	1.1

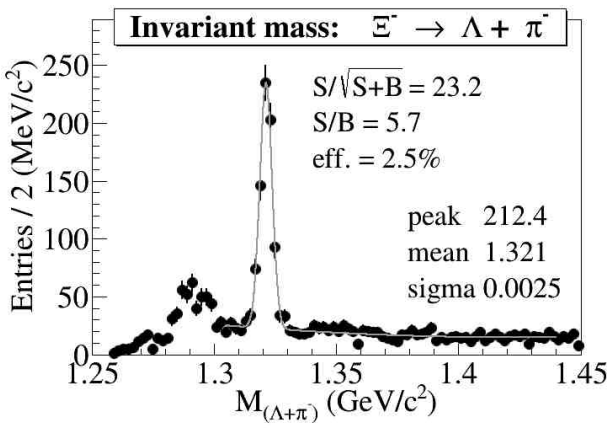

Fig. 9. Reconstructed invariant mass of Λ candidate and π^-.

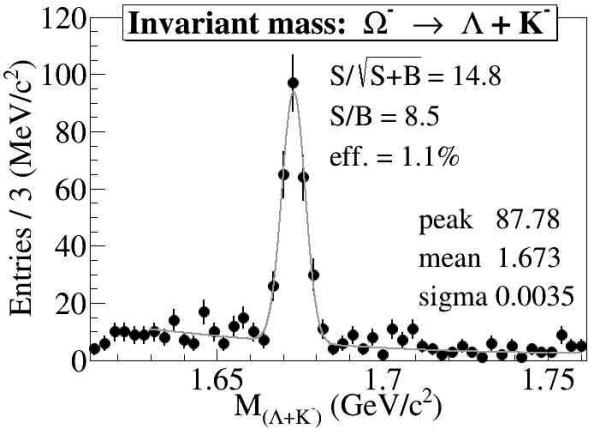

Fig. 10. Reconstructed invariant mass of Λ candidate and K^-.

were introduced to find the significance maximum for this cascade decay topology.

Reconstruction of Ω^- hyperons

The results (Tab. 3 and Fig. 10) have been obtained for $5 \cdot 10^5$ central events, corresponding to about 28 minutes of data taking time at NICA. Here the necessity of suppressing a larger combinatorial background and a requirement to have a sufficient significance of the signal results in stronger cuts and lower efficiencies. Also, as in the case of lighter hyperons we observed a large drop in the overall reconstruction efficiency when the low-p_t cut-off of decay products is increased from 0.1 to 0.2 GeV/c. Therefore, the MPD detector ability of reconstructing very low momentum particles (at least, down to $p_t = 0.1$ GeV/c) is of crucial importance for measurements of multistrange hyperons.

Table 4. Expected particle yields in central Au+Au collisions for 10 weeks of running time

Particle	Λ	Ξ^-	Ω^-
Expected yield	$5.8{\cdot}10^9$	$2.9{\cdot}10^7$	$1.4{\cdot}10^6$

SUMMARY

We have performed a simulation study of the MPD detector capabilities of reconstructing hyperons (Λ, Ξ^- and Ω^-) in central Au+Au collisions at $\sqrt{s}$ =9A GeV. The UrQMD event generator was used as the input for a study of the MPD detector set-up comprising the Time-Projecting Chamber (TPC) and barrel Time-Of-Flight system. Particle identification was achieved by combining the energy loss (from TPC) and time-of-flight (from TOF) measurements. A special procedure aimed at the maximization of the significance of the reconstructed invariant mass peak was applied for hyperons resulting in the observed signal-to-background ratio for $S/B \gtrsim 6$. The invariant mass resolution of $\approx$3 MeV/c^2 was achieved. Based on the results of this study and model predictions, we have estimated the expected yields of particle species under interest for 10 weeks of data taking (see Table 4).

REFERENCES

[1] J. Rafelski and B. Muller, *Phys. Rev. Lett.* **48**, 1066 (1982).

[2] K.U. Abraamyan et al., *Nucl. Instrum. Meth. A.* **628**, 99 (2011).

[3] http://nica.jinr.ru.

[4] *Searching for a QCD Mixed Phase at the Nuclotron Based Ion Collider Facility (NICA White Paper)*, https://indico.cern.ch/event/275003/contribution/1/material/paper/0.pdf.

[5] http://nica.jinr.ru/files/CDR_MPD/MPD_CDR_en.pdf.

[6] http://mpd.jinr.ru/.

[7] http://urqmd.org/.

[8] R. Fruehwirth, *Nucl. Instr. and Meth. A.* **262**, 444 (1987).

[9] R. Luchsinger and Ch. Grab, *Comp. Phys. Comm.* **76**, 263 (1993).

РЕКОНСТРУКЦИЯ НА ХИПЕРОНИ В МНОГОЦЕЛЕВИЯ ДЕТЕКТОР MPD (NICA)

Д. Сувариева, М. Илиева, В. Колесников, В. Васендина, Ал. Зинченко

Лаборатория по високи енергии, Обединен институт за ядрени изследвания,
ул. "Академик Балдин" № 4, 141980 Дубна, Московски регион, Русия

(Резюме)

Идентификация и реконструкция на странни частици е една от най-важните задачи на всеки експеримент с тежки йони, така е и за нашият проект NICA. Те биха могли да предоставят основна информация за горещата и плътна барионна материя. Представени са резултати от реконструкцията на ламбда Λ, кси Ξ^- и омега Ω^-) хиперони, които са получени на базата на Монте Карло симулации за сблъсъци на злато - злато, при енергии енергии – 9A GeV. За да се изследва създаването на ядрени фрагменти от такива сблъсъци се използва и генераторът UrQMD. Показано е, че стартовата версия на MPD и развитите методи, алгоритми и софтуер ще предоставят добра възможност за изследване на странни частици на ускорителния комплекс NICA (разрешение по маса 2-3 MeV/c^2).